



## Green and selective oxidation reactions catalyzed by kaolinite covalently grafted with Fe(III) pyridine-carboxylate complexes

Emerson H. de Faria<sup>a,\*</sup>, Gustavo P. Ricci<sup>a</sup>, Liziane Marçal<sup>a</sup>, Eduardo J. Nassar<sup>a</sup>, Miguel A. Vicente<sup>b</sup>, Raquel Trujillano<sup>b</sup>, Antonio Gil<sup>c</sup>, Sophia A. Korili<sup>c</sup>, Katia J. Ciuffi<sup>a,\*</sup>, Paulo S. Calefi<sup>a</sup>

<sup>a</sup> Universidade de Franca, Av. Dr. Armando Salles Oliveira, Parque Universitário, 201, 14404-600 Franca, SP, Brazil

<sup>b</sup> Departamento de Química Inorgánica, Facultad de Ciencias Químicas, Universidad de Salamanca, Plaza de la Merced, S/N, 37008 Salamanca, Spain

<sup>c</sup> Department of Applied Chemistry, Public University of Navarre, Campus of Arrosadia, Pamplona, Spain

### ARTICLE INFO

#### Article history:

Received 2 June 2011

Received in revised form

21 November 2011

Accepted 23 November 2011

Available online 3 January 2012

#### Keywords:

Kaolinite

Heterogeneous catalysis

Fe(III)–picolinates and dipicolinates

Oxidation reactions

Baeyer–Villiger

### ABSTRACT

The immobilization of Fe(III) picolinate and Fe(III) dipicolinate complexes on kaolinite furnished heterogeneous catalysts, whose catalytic activity was evaluated. The precursor materials were kaolinite grafted with picolinic (Ka-pa) and dipicolinic (Ka-dpa) acids obtained by melting of the pyridine carboxylic acids. To obtain the catalysts Fe(Ka-pa)-*n* and Fe(Ka-dpa)-*n* (*n* = 1, 2, or 3 is the ligand/Fe ratio), the precursors were suspended in Fe<sup>3+</sup> solutions with cation/ligand ratios of 1:1, 1:2, or 1:3. The resulting materials were characterized by thermal analyses (simultaneous TG/DTA), X-ray diffraction, UV/vis and infrared spectroscopies, and transmission electron microscopy. The grafted complexes were employed as heterogeneous catalysts in the epoxidation of cis-cyclooctene to cis-cyclooctenoxide and in the oxidation of cyclohexane to cyclohexanol and cyclohexanone at ambient temperature and pressure. Hydrogen peroxide was used as oxygen donor at a catalyst/oxidant/substrate molar ratio of 1:300:100. Fe(Ka-pa)-*n* catalysts were very efficient for cis-cyclooctene epoxidation (38% conversion). For cyclohexane oxidation, Fe(Ka-dpa)-*n* was 100% selective for cyclohexanone formation, with substrate conversion of 14%. This last series of catalysts was also very effective in the Baeyer–Villiger reaction, with 60% substrate conversion and 100% selectivity for  $\xi$ -caprolactone. After reuse (5 times), the catalysts still led to high substrate conversion.

© 2011 Elsevier B.V. All rights reserved.

### 1. Introduction

Catalysis is the base of countless chemical processes that transform crude and cheap raw material into products of high economic value and extreme importance for humankind. Moreover, catalytic technologies are of utmost importance for environmental sustainability [1]. The most commonly employed catalytic routes make use of metallic catalysts to improve reaction rate and selectivity [2–4]. Traditional hydrocarbon oxidation uses vast amounts of highly toxic inorganic compounds such as potassium permanganate and dichromate. According to Hill [5], the ideal “green” oxidizing systems are molecular oxygen and hydrogen peroxide in combination with recyclable catalysts in non-toxic solvents. Immobilization of metal complexes on inorganic supports such as clay minerals has led to the successful preparation of efficient and selective heterogeneous catalysts for the oxidation of organic substrates. In this

context, layered materials have been successfully employed as catalytic supports in hydrocarbon oxidation, enhancing the catalytic activity of the metal complex and promoting product selectivity [6]. Recently, catalysts containing iron or manganese porphyrins as active phases have been reported [7–12].

Environmentally friendly catalytic reactions have increasingly drawn the attention of scientists, environmentalists, and politicians worldwide [13], as these reactions lead to low waste generation, not to mention that they enable the use of mild conditions and the design of highly selective and active heterogeneous catalysts, which is desirable in an age when the control of environmental pollution and the reduction of energy consumption are mandatory (sustainable chemistry). Some zeolites and natural clays (montmorillonite, saponite, kaolinite) display interesting catalytic properties, and the use of modified clays as catalysts has been encouraged because they matches the sustainable chemistry conditions. Layered materials were already employed as catalysts in the beginning of the petrochemical industry, and the first hydrocracking process was based on acid-treated clays [2]. However, it is believed that synthetic systems consisting of functionalized or intercalated clays can overcome the performance of such materials. Indeed, processes that promote the structural modification of clays can tailor the characteristics of the catalysts in such a way that

\* Corresponding authors.

E-mail addresses: [eh.defaria@unifran.br](mailto:eh.defaria@unifran.br) (E.H. de Faria), [ciuffi@unifran.br](mailto:ciuffi@unifran.br) (K.J. Ciuffi).

their activity and selectivity in oxidation reactions can be enhanced [14–17]. Some advantages of using functionalized clays are:

- The possibility of achieving uniform intercalation or grafting of the active species during the synthesis (without impurities).
- The large-scale production of catalysts with homogeneous chemical composition and catalytic properties.
- Complexation of highly catalytically active transition metal ions such as  $\text{Fe}^{3+}$ ,  $\text{Co}^{3+}$ , and  $\text{Mn}^{3+}$  species with functional groups located in the basal space of clays, giving rise to efficient, selective heterogeneous catalysts [18–20].

As already commented, layered materials represent an interesting opportunity for the development of new catalysts [2]. In this context, kaolinite, with theoretical formula  $\text{Al}_2\text{Si}_2\text{O}_5(\text{OH})_4$ , is a typical example of layered structure, since it is formed by combining sheets of  $\text{SiO}_4$  tetrahedra (T) and  $\text{Al}(\text{OH})_6$  octahedra (O) in a 1:1 proportion [21,22]. The use of layered materials as heterogeneous catalysts is based on their surface activity, which can promote a large variety of organic reactions such as Diels–Alders cyclization of organic compounds, and oxidation reactions of organic compounds such as *cis*-cyclooctene, cyclohexane and the Baeyer–Villiger oxidation [23].

The combination of organic and inorganic constituents on the atomic/molecular scale gives rise to materials with singular properties, thereby allowing for adjustable applications. Such materials include those obtained by clay mineral intercalation or functionalization, whose morphological characteristics enable superficial and interplanar chemical modifications that lead to the effective immobilization of complexes, such as metalloporphyrins, organic molecules, polymers, and alkoxides [24,25]. The materials resulting from immobilization processes have followed a fast growing interest in functional properties and applications in many areas of science and technology such as catalysis, adsorption, conductors, and optical and photoactive materials [26–29]. Recently our research group has reported the functionalization of natural kaolinite with pyridine-carboxylic acids, alkoxides, and ironporphyrins by the soft-guest displacement methodology.

Catalytic oxidation reactions generally involve the use of soluble salts or complexes in the presence of oxidants like  $\text{O}_2$ ,  $\text{H}_2\text{O}_2$ , iodobenzene (PhIO), or  $\text{KMnO}_4$ . The catalytic oxidation of the C–H bonds of alkanes at ambient temperature and pressure has attracted extensive and ongoing interest worldwide, by using systems that can mimic the dioxygen activation induced by iron-containing biological systems such as cytochrome P-450 [30].

Over the last decade the search for efficient and environmentally friendly oxidation procedures that could be used to develop green processes for many kinds of oxidation reactions has been intensified. This can be achieved by employing clean oxidants like hydrogen peroxide, which is considered as an ideal oxidant because of its high active oxygen content, availability, and non-toxicity. Moreover, it is considered to be non-polluting, since it produces only water as product [31]. Oxidations with hydrogen peroxide are highly atom-economic, and it is a safe, readily available and cheap reagent.

Traditionally ironporphyrins have been reported as efficient and selective catalysts for hydrocarbons oxidation and they are good biomimics of cytochrome P-450 [18,25,30–33]. However, their use is not always feasible on an industrial scale, because their synthesis demands arduous purification procedures and chlorinated solvents are employed in their syntheses. This encouraged us to investigate the potential of the catalyst prepared herein as biomimetic catalysts for hydrocarbons oxidation, using the clean oxidant hydrogen peroxide.

Other reaction considered in this work is Baeyer–Villiger oxidation. From the historical report by Baeyer and Villiger of the

oxidation of menthone and tetrahydrocarvone to their corresponding lactones using monopersulfuric acid ( $\text{H}_2\text{SO}_5$ ) as oxidant, this versatile reaction has become one of the most applied industrial processes [34,35], being useful for the preparation of chemical, agrochemical and pharmaceutical compounds [36]. Catalysts commonly employed for this oxidation are zeolites and aluminas [37], while clays as montmorillonite [35] and kaolinite [25] have also been utilized.

Traditionally, peracids are employed as oxidants in the Baeyer–Villiger reaction. However, it is evident that these oxidants are troublesome for large-scale utilization. One of the factors that make a catalyst efficient for the Baeyer–Villiger reaction is its ability to increase the electrophilicity of the peroxide. This activation enhances the oxidant's activity toward electron deficient centers, such as carbonyls. Metals such as Ti, V, Mo, and W may form peroxy complexes in the presence of  $\text{H}_2\text{O}_2$ , but these have an electrophilic nature, which justifies their activity in hydrocarbon oxidation. However, the nucleophilic attack of the peroxy group to carbonyl groups is improbable. Jacobson et al. [38] were the first to report on the nucleophilic reactivity of peroxy complexes containing transition metals. These authors employed the Mo(VI)-dipicolinate complex in the oxidation of cyclopentanone at 60 °C and achieved 93% product yield after 24 h. Recently, many research groups have investigated this reaction in the presence of various catalysts, like natural and/or synthetic clays, alumina, and transition metals supported on different matrices [25,35–38].

This paper reports the immobilization of Fe(III)–picolinate and Fe(III)–dipicolinate on kaolinite. The grafted complexes were used as heterogeneous environmental-friendly catalysts in the epoxidation of *cis*-cyclooctene to *cis*-cyclooctenoxide, in the oxidation of cyclohexane to cyclohexanol and cyclohexanone, and in the Baeyer–Villiger oxidation of cyclohexanone to  $\xi$ -caprolactone, using hydrogen peroxide as oxidant. The nature of the catalysts and the catalytic routes studied are summarized in Fig. 1.

## 2. Experimental

### 2.1. Catalyst preparation

#### 2.1.1. Functionalization of natural kaolinite with Fe(III)–picolinate and Fe(III)–dipicolinate

The kaolinite employed in this work came from the municipality of São Simão in the State of São Paulo, Brazil, and was kindly supplied by the mining company Darcy R.O. Silva & Cia. It belongs to the ball-clay type, known for its fine granulometry and for being rich in hexagonal kaolinite. Kaolinite was purified by dispersion in water, followed by sedimentation, according to Stock's law and using the procedure previously described by us [25,27–29]. The structural formula of purified kaolinite is  $\text{Si}_{2.0}\text{Al}_{1.96}\text{Fe}_{0.03}\text{Mg}_{0.01}\text{K}_{0.02}\text{Ti}_{0.03}\text{O}_{7.06}$  [27].

Grafted kaolinite-pyridine carboxylic acids compounds were prepared according to the methodology described by de Faria et al. [27]. Briefly, kaolinite was first expanded with dimethylsulfoxide, the resulting complex, designated Ka-DMSO, has the stoichiometry  $\text{Ka}(\text{DMSO})_{0.45}$  (Ka denotes the cell-formula of kaolinite reported above). This precursor was heated for 40 h in the presence of melted acid (picolinic or dipicolinic) in a 1:5 molar ratio, and then the resulting materials were washed with ethanol and oven-dried at 80 °C. They were designated Ka-pa and Ka-dpa when derived from picolinic and dipicolinic acids, respectively. To obtain the derivate Fe containing catalysts, Ka-pa and Ka-dpa were suspended in a 0.1 mol/L  $\text{Fe}^{3+}$  solution, using the volumes needed to reach ligand/Fe ratios, denoted as *n*, of 1.0, 2.0, or 3.0, and the mixture was stirred at 55–60 °C for 3 h. The suspensions were centrifuged, and the resulting solids were washed with ethanol five times.

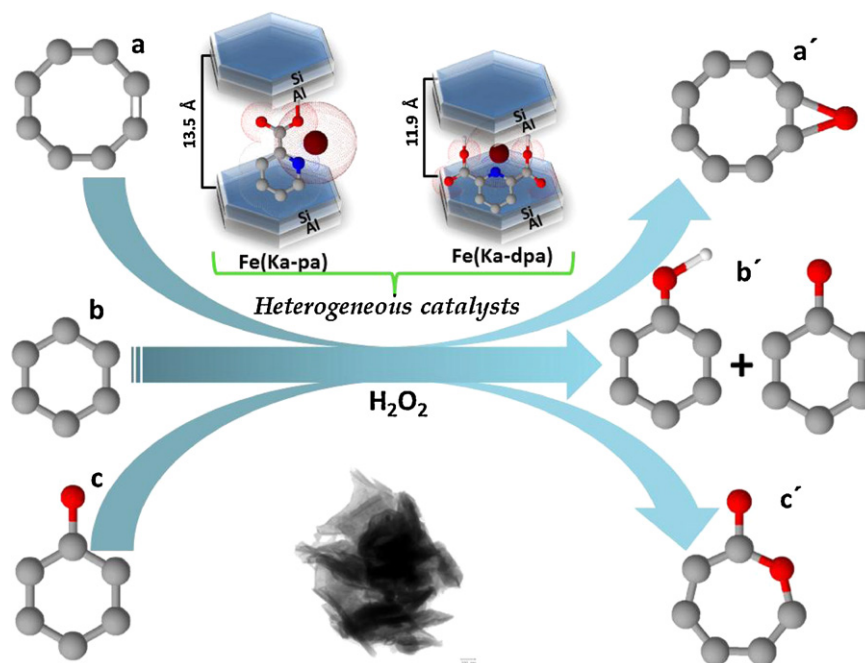


Fig. 1. Schematic representation of catalytic oxidations by Fe(III)-pyridine carboxylic complexes grafted on kaolinite.

The catalysts obtained were designated by a general nomenclature Fe(Ka-pa)-*n* and Fe(Ka-dpa)-*n* when reference is made to a complete series, and specifying the value of *n* when reference is made to a given sample.

### 2.1.2. Synthesis of isolated Fe(III)-picolinate and Fe(III)-dipicolinate complexes – homogenous catalysts

The Fe(III) picolinate and dipicolinate complexes were prepared according to the methodology described by Amani et al. [39]. Picolinic (500 mg,  $4.06 \times 10^{-3}$  mol) or dipicolinic (500 mg,  $2.99 \times 10^{-3}$  mol) acid in 0.1 mol/L HCl solution (20 mL) was added to a solution of  $\text{FeCl}_3 \cdot 6\text{H}_2\text{O}$  (439 mg,  $1.62 \times 10^{-3}$  mol or 324 mg,  $1.19 \times 10^{-3}$  mol, respectively) in distilled water, and the resulting solution was stirred at 55–60 °C for 3 h. The complexes were precipitated, and then recrystallized from acetonitrile, yielding 97% and 95% from the reactions with picolinic and dipicolinic acid, respectively. The resulting complexes were designated Fe(pa)<sub>3</sub> and Fe(dpa)<sub>3</sub>, respectively.

## 2.2. Characterization techniques

The X-ray diffractograms of the solids were acquired on a Siemens D-500 diffractometer operating at 40 kV and 30 mA (1200 W), using filtered Cu K $\alpha$  radiation, varying the angle  $2\theta$  from 2° to 65°. All the analyses were processed at a scan speed of 2°/min.

Infrared absorption spectra were obtained on a Perkin-Elmer 1739 spectrophotometer with Fourier transform, using the KBr pellet technique.

UV–vis spectra were recorded in the 200–800 nm range on a HP 8453 Diode Array Spectrophotometer. Spectra of the solid samples were recorded in a quartz cell with 0.1 cm path length, in ethanol suspension.

Thermal analyses (TG/DSC) were carried out in a TA Instruments SDT Q600 Simultaneous DTA-TGA thermal analyzer, in the temperature range between 25 and 1100 °C, at a heating rate of 20 °C/min and air flow of 100 mL/min.

Element chemical analysis was carried out at *Servicio General de Análisis Químico Aplicado* (University of Salamanca) by atomic

absorption after dissolving the samples in nitric acid, in a Mark-II ELL-240 instrument.

Transmission electron microscopy (TEM) was performed using a Zeiss-902 microscope over samples ground and dispersed in ethanol by using an ultrasonic apparatus; then, a drop of the suspension was placed in a Cu grid and air dried before the study.

Products from the catalytic oxidation reactions were identified using a HP 6890 Series GC System gas chromatograph (with a flame ionization detector) equipped with a capillary column HP-INNOWax-19091N-133, polyethylene glycol length 30 m, internal diameter 0.25  $\mu\text{m}$ ). The products were quantified using a calibration curve obtained with a standard solution, and the conversion was based on substrate. Technical error: about  $\pm 1\%$ .

All solvents and reagents were purchased from Mallinckrodt, Aldrich, or Acros Organics and were of commercial grade, unless otherwise stated. Dichloromethane (DCM) was suspended on anhydrous  $\text{CaCl}_2$  for 2.5 h, filtered, distilled over  $\text{P}_2\text{O}_5$ , and kept over 4 Å molecular sieves. *cis*-Cyclooctene, cyclohexane, cyclohexanol, and cyclohexanone were purified on a basic alumina column immediately before use. Hydrogen peroxide (solution in water) was donated by *Peróxidos do Brasil SA* and was iodometrically titrated before use (indicating a  $\text{H}_2\text{O}_2$  content of 60 wt.%) [40].

## 2.3. Catalytic activity

### 2.3.1. Oxidation of *cis*-cyclooctene and cyclohexane by hydrogen peroxide

Catalytic oxidation reactions were carried out in a 2 mL glass reactor equipped with a magnetic stirrer. In a typical heterogeneous catalysis reaction, 10 mg of the catalyst Fe(Ka-pa)-*n* or Fe(Ka-dpa)-*n* were suspended in 1 mL of the solvent mixture (dichloroethane/acetonitrile, 1:1, v/v), and the substrate (*cis*-cyclooctene (125  $\mu\text{L}$ ) or cyclohexane (100  $\mu\text{L}$ )) was added. Molar ratio of catalyst/ $\text{H}_2\text{O}_2$ /substrate was 1:300:100 (the molar mass of each catalyst was calculated from its structural formula). The oxidation reactions were carried out during a controlled time interval of 2, 4, 24, or 48 h. The reaction products were analyzed by gas chromatography using the internal standard method.

At the end of the reaction, the Fe(Ka-pa)-*n* and Fe(Ka-dpa)-*n* catalysts were recovered by centrifugation, washed in dichloroethane and dried for 3 h at 60 °C before being used again in a further cis-cyclooctene or cyclohexane oxidation reaction.

The concentration of hydrogen peroxide after the oxidation reactions was measured by iodometric titration to determine the real efficiency of hydrogen peroxide [40].

### 2.3.2. Oxidation of cis-cyclooctene and cyclohexane by iodobenzene

Iodobenzene (PhIO) was obtained through hydrolysis of iodobenzene diacetate [40], and the purity of the obtained compound was evaluated by iodometric titration [41]. PhIO (0.023 mmol) was added to a 2.0 mL vial sealed with a Teflon-coated silicone septum containing the catalyst (10 mg) and 1,2-dichloroethane (1 mL). cis-Cyclooctene, cyclohexane, cyclohexanol, all of them previously purified on alumina column, or cyclohexane were added as substrate (1.15 mmol) and di-*n*-butyl ether was employed as internal standard (10 μL). The reaction products were analyzed by gas chromatography (GC). The products were quantified using a calibration curve obtained with a standard solution, and the yield was based on oxidant.

### 2.3.3. Baeyer–Villiger (BV) oxidation of cyclohexanone

The BV oxidation reaction was carried out in a 4.0 mL glass reactor. A 50 μL portion of cyclohexanone (0.48 mmol), 850 μL benzonitrile (7.95 mmol), 5.0 μL di-*n*-butyl ether (2.94 μmol), 176 μL of 60 wt.% (4.53 mmol) or 352 μL (4.53 mmol) of 30 wt.% hydrogen peroxide and 20 mg of the catalysts were added to the reactor; the mixture was then heated to 80 °C and stirred for 48 h. At the end of the reaction, the catalysts were recovered, dried for 3 h at 60 °C and used again in a further Baeyer–Villiger oxidation reaction.

In both cases, control reactions were carried out for all the oxidation reactions in the absence of catalysts, in absence of oxidants or using kaolinite grafted with picolinic and dipicolinic acids but without containing Fe(III), while the control test to Baeyer–Villiger oxidation reactions was conducted without benzonitrile using as solvent a mixture of dichloroethane/acetonitrile, 1:1 (v/v), the molar ratio of catalyst/oxidant/substrate was maintained.

The supernatant was separated from the catalysts by centrifugation and maintaining the supernatant of this reaction on a glass reactor until 24 h, aftermost the possible products formed were quantified by GC. Indeed, this simple test can give evidence of the leaching of active Fe(III)-species from solid to supernatant.

## 3. Results and discussion

### 3.1. Characterization of kaolinite functionalized with Fe(III) complexes

The X-ray diffractograms of the grafted solids derived from kaolinite are presented in Figs. 2 and S1 (Supplementary material). The solids intercalated with picolinic and dipicolinic acids displayed basal spacings of 13.50 and 11.90 Å, respectively, in both cases also presenting a small effect at 7.20 Å, characteristic spacing of non-intercalated kaolinite [27]. The incorporation of Fe(III) did not affect the basal distance of Ka-pa solids, although the peak characteristic of expanded kaolinite decreased in intensity, and that from non-expanded kaolinite increased, suggesting that part of the ligand may leave the interlayer region to form complexes out of it, and even that complexation process in water medium promotes the disorder of kaolinite layers. This mainly happened in the Fe-(Ka-pa)-3 solid, which has the higher Fe/pa ratio, in which two new peaks characteristic of Fe-pa complexes are observed at 9.30 and 5.60 Å. This logically provokes an increase in the intensity of the

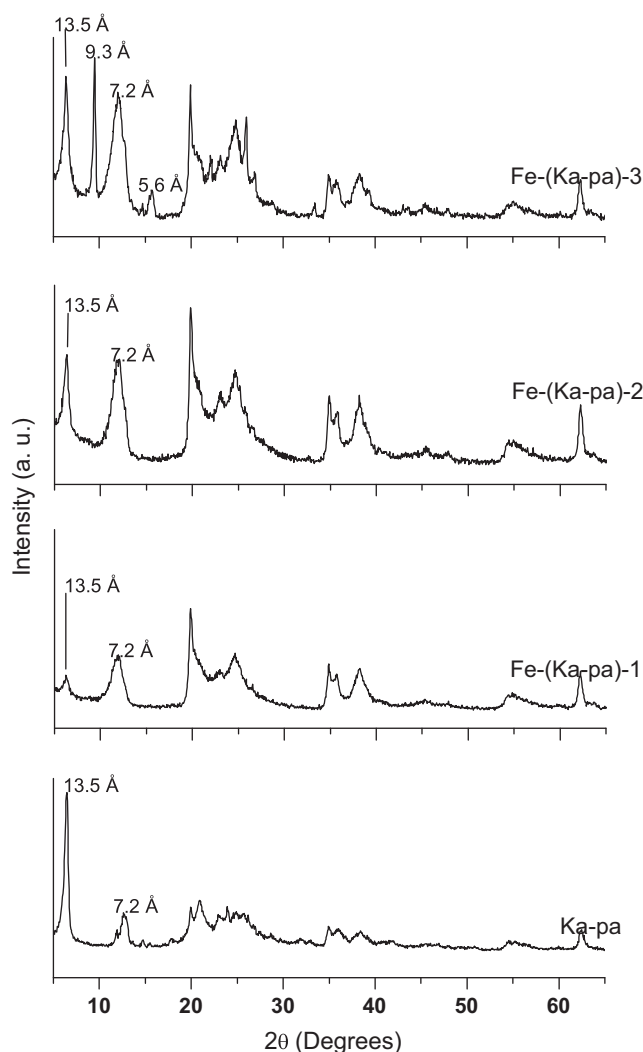


Fig. 2. X-ray powder diffraction patterns ( $2\theta = 2\text{--}65^\circ$ ) of the precursor Ka-pa (a), and the catalysts Fe(Ka-pa)-1 (b), Fe(Ka-pa)-2 (c) and Fe(Ka-pa)-3 (d).

peak of non-expanded kaolinite. In the case of Ka-dpa series, the basal spacing decreased from 11.90 Å in the dpa-expanded kaolinite to 11.40 Å in the Fe-containing solids, which suggests a more planar arrangement of dpa molecules when complexing Fe(III) ions. At the same time, new reflections are observed, for all the solids in this series, at 8.39 Å, assigned to the formation of a tubular phase of kaolinite due to a curling process in the layers and at 6.30 Å, 5.90 Å, and 5.50 Å, assigned to the 002 reflection present in solids with high crystallinity. Recently, curling of single layers or even small stacks of layers of kaolinite after intercalation and functionalization has been reported, resulting in the so-called “halloysite-like”, tubular, or scroll-like kaolinite. As for kaolinite functionalized with dipicolinic acid and complexed with Fe(III), peaks at 8.39, 6.28, 5.95 and 5.48 Å were detected, ascribed to the presence of the kaolinite tubular phase [18,32,33,42]. This phase is obtained due to interaction between the Fe(III)-dipicolinate complex and the inorganic matrix, thereby reducing the interactions between the layers and promoting their curling [18,32,33,42]. XRD patterns revealed that the peak at 7.14 Å, characteristic of pure kaolinite remaining from the synthesis, is displaced to 7.20 Å in the case of the kaolinite derivatives Ka-DMSO, Ka-pa, and Ka-dpa, and this peak becomes broad after iron coordination because of the presence of water molecules coordinated to the Fe(III) complexes located in the



**Table 1**  
Interlayer basal space,  $d_{001}$ , variation in basal space ( $\Delta d$ ), and intercalation ratio ( $\alpha$ ) of the materials prepared in this work.

Sample	$d_{001}$ (Å)	$\Delta d$ (Å)	$\alpha^*$ (%)
Ka	7.14	–	–
Ka-DMSO	11.20	4.06	98
Ka-pa	13.50	6.36	92
Fe(Ka-pa)-1	14.20	7.06	44
Fe(Ka-pa)-2	13.90	6.76	51
Fe(Ka-pa)-3	13.90	6.76	51
Ka-dpa	11.90	4.76	86
Fe(Ka-dpa)-1	11.50	4.36	80
Fe(Ka-dpa)-2	11.50	4.36	68
Fe(Ka-dpa)-3	11.35	4.21	66

\* The intercalation ratio ( $\alpha$ ) was determined according to the relative intensities of the peaks relative to the basal space  $d_{001}$  in relation to the characteristic reflection of purified kaolinite.  $\alpha = I/(I + I_0)$ ,  $I$  = intensity  $d_{001}$  of the products,  $I_0$  = intensity  $d_{001}$  of the characteristic reflection of non-reacted kaolinite.

interlayers of kaolinite. Table 1 summarizes the results from XRD patterns of grafted derivatives after complexation with Fe(III).

The intercalation ratio, that is, the percentage of layers intercalated, decreased from 92% in the Ka-pa solid to 44–51% in the Fe-containing solids in this series. Although the intercalation ratio is slightly lower in the parent solid of Ka-dpa series (86%), the amount of layers intercalated in the Fe-containing solids was clearly higher, 66–80% (Table 1). This suggests that the presence of  $\text{Fe}^{3+}$  ions induces a partial lixiviation of the intercalated ligands, forming complexes located out of the interlayer region. This is

justified by the strong affinity of the ligands for Fe(III), as the entrance of Fe(III) to the interlayer region is relatively difficult, some picolinate anions go out of this region to form the very stable complexes. On the other hand, it became evident that lixiviation depends on the number of carboxylate groups present on the functionalized kaolinite. Indeed, the hybrids Ka-dpa were more stable against lixiviation, probably because the dipicolinate anions, larger than the picolinate ones, have more difficulties to leave the interlayer region, while Ka-pa series showed higher lixiviation of the ligands out of the layers.

The formation of kaolinite nanotubes (or scroll-like structure) was confirmed by TEM (Fig. 3). The micrographs showed that the tubes have different diameters, probably because the curling process of kaolinite was incomplete. Nakagaki et al. have assigned the formation of nanotubes in silanized kaolinite intercalated with a porphyrin to the strong interaction between the silanized kaolinite layer and the porphyrin [18,32,33]. The intercalation of organic moieties hinders or reduces the formation of hydrogen bonds between silica (Si–O) and alumina (Al–OH) in kaolinite layers, thereby promoting curling of the layers. It is known that curling process is favored when the hydrogen bonds of the kaolinite structure are weakened by the intercalation or grafting of strongly polar molecules such as amines, alcohols, etc. Gardolinski and Lagaly have described the curling of kaolinite layers when intercalated with large amine molecules (*n*-alkylamine, octadecylamine) [43]. The preparation of halloysite-like kaolinite is more efficient in materials with a high degree of disorder between the layers, thus being favored for hybrid compounds.

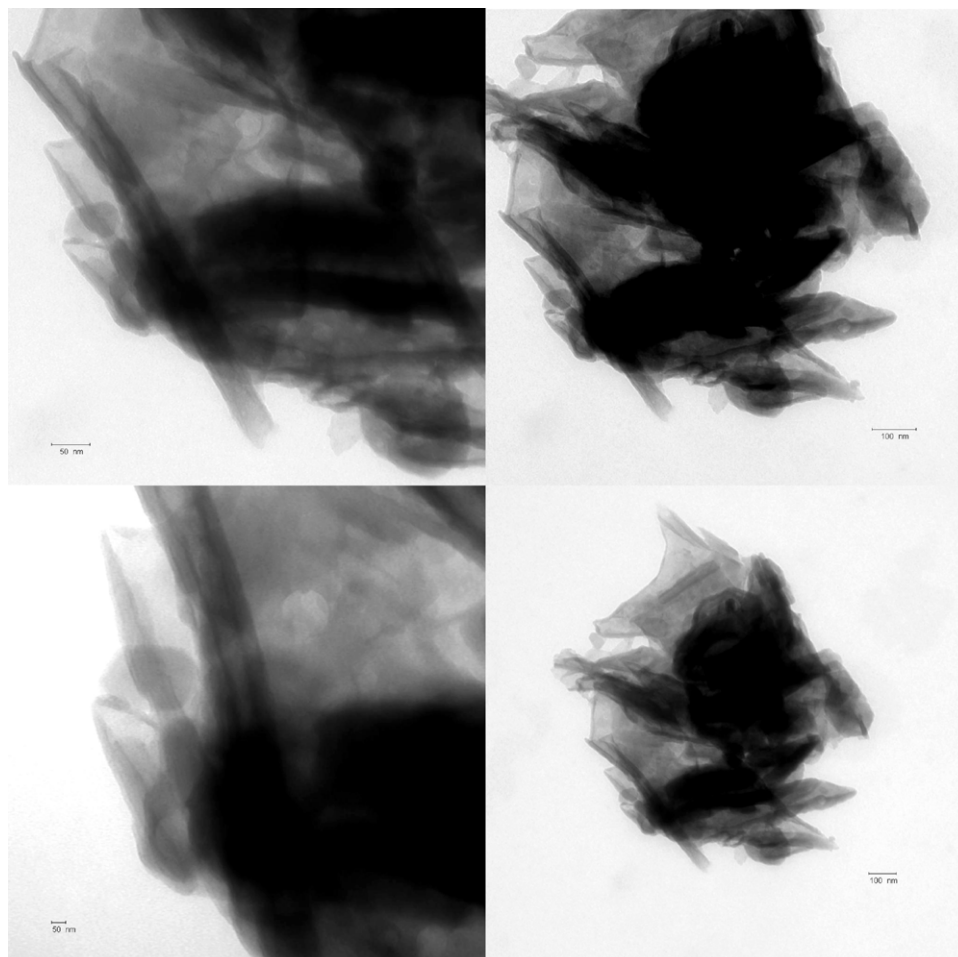


**Fig. 3.** Transmission electron micrographs of the Fe(Ka-dpa)-3 materials showing the halloysite-like structure with magnifications of 25,000 $\times$ .

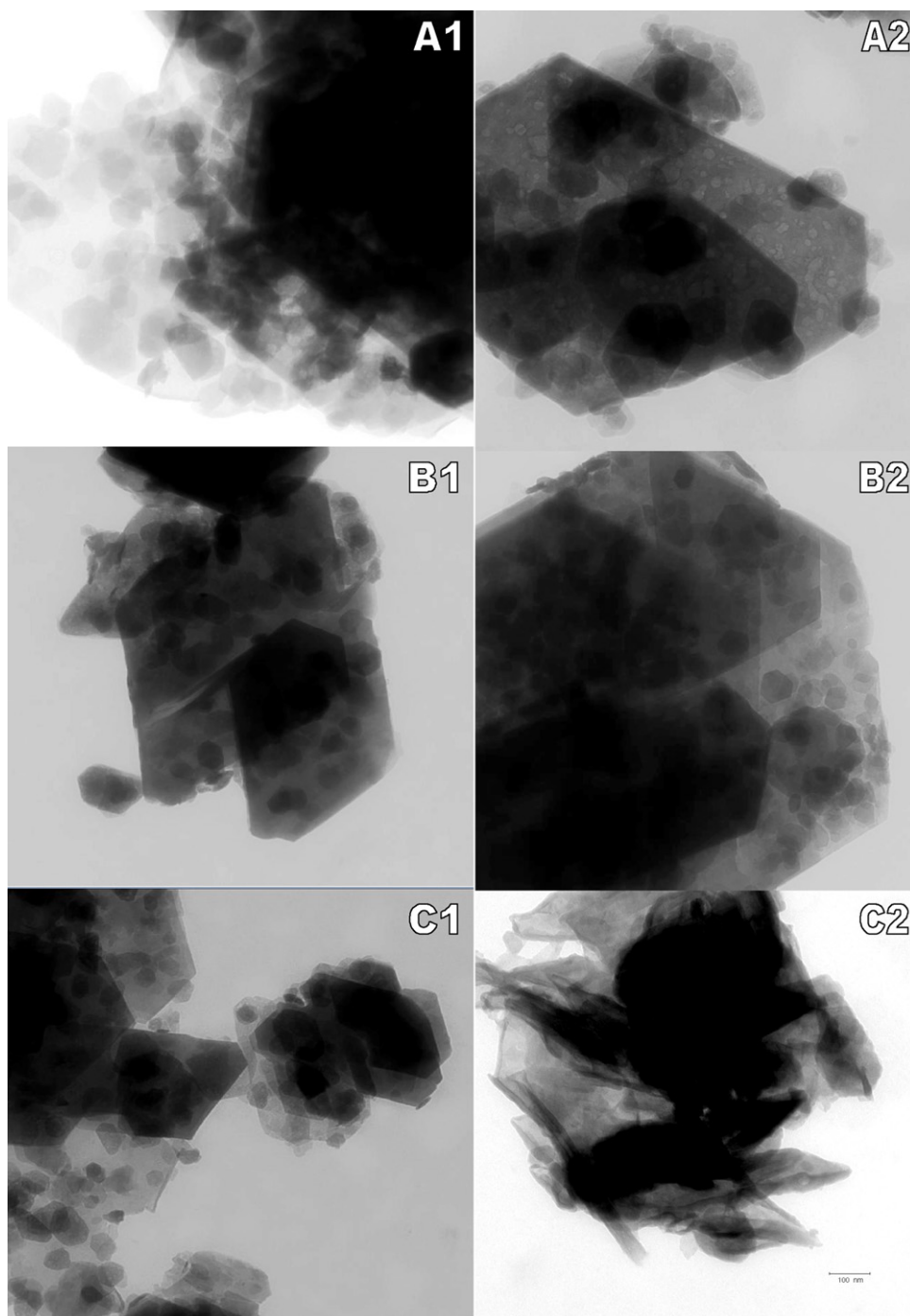


**Fig. 4.** Transmission electron micrographs with 25,000 $\times$  magnification of the precursors Ka-pa (A.1) and Ka-dpa (A.2), of the catalysts obtained after complexation in ethanolic medium: Fe(Ka-pa)-3[eth] (B.1) and Fe(Ka-dpa)-3[eth] (B.2), and of the catalysts obtained after complexation in aqueous medium: Fe(Ka-pa)-3[H<sub>2</sub>O] (C.1) and Fe(Ka-dpa)-3[H<sub>2</sub>O] (C.2).

TEM micrographs also evidenced the presence of some crystals of pure kaolinite with unmodified hexagonal structure, which is in agreement with the maintenance of the 7.2 Å – reflection in the XRD patterns.

Thus, the curling process in our solids may be induced by the presence of water and by the coordination of Fe(III) to the pa and dpa anions grafted to the kaolinite layer. With the aid of the software Orion 6.53 (free available at <http://www.orionmicroscopy.com/demo.php>), the internal and external diameters of the nanotubes were determined to be 30 nm and 80 nm, respectively, and their thickness was found to be 25 nm.

As several authors have attributed kaolinite curling to the presence of water molecules, this influence was studied by synthesizing one of the solids in each series in the absence of water. The samples were designated as Fe-(Ka-pa)-3[eth] and Fe-(Ka-dpa)-3[eth], according to the ethanolic reaction medium. Fig. 4 depicts the TEM micrographs of these samples, which clearly reveals that there was no formation of the tubular phase with halloysite-like structure in ethanolic medium (in this figure, for avoiding confusion, [H<sub>2</sub>O] is added to the name of the samples prepared in aqueous medium). This confirmed that the curling process was really promoted by the presence of water molecules and not by formation of pa- or

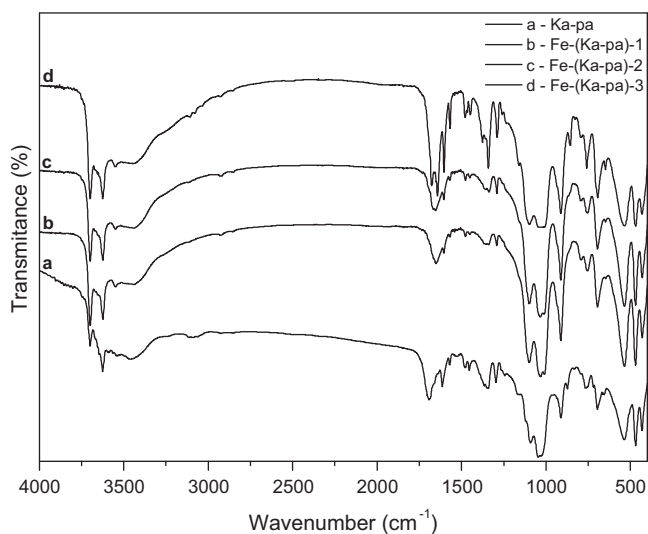


**Fig. 5.** Infrared spectra of the compound Ka-pa (a), and the catalysts Fe(Ka-pa)-1 (b), Fe(Ka-pa)-2 (c) and Fe(Ka-pa)-3 (d).

dpa-Fe(III) complexes. In aqueous medium, two factors may have contributed to the formation of the tubular phases: the presence of water molecules and the reduced cohesion force between kaolinite layers after insertion of pa and dpa molecules.

Figs. 5 and S2 show the FTIR spectra of Ka-pa, and Ka-dpa precursors, and of the catalysts obtained after complexation with Fe(III), the assignment of the bands is summarized in Table S1 (Supplementary material). The infrared spectra of parent kaolinite displayed four bands in the 3500–3800  $\text{cm}^{-1}$  region (3694, 3668, 3650, 3618  $\text{cm}^{-1}$ ), which can be assigned to the stretching of the inter- and intralamellar hydroxyls [27]. The displacement of these bands evidenced the intercalation of molecules in this region. In Ka-pa and Ka-dpa solids, the bands typical of the asymmetric and symmetric stretching of the carboxylic acid groups were also observed at 1689, 1566, and 1478  $\text{cm}^{-1}$  [27–29].

After complexation with Fe(III), the bands attributed to the stretching of C=N, C=O and C–H bonds shifted from 1649, 1615, 1570, 1480–1454, 1345, and 1297  $\text{cm}^{-1}$  to 1678, 1642, 1604, 1499–1480, and 1290  $\text{cm}^{-1}$ , thereby confirming the coordination of Fe(III) to the N atom and the carboxylate group of the picolinate anions grafted on kaolinite. The band observed at 1705  $\text{cm}^{-1}$  is ascribed to the C=O stretching vibration of the pa carboxylic acid group coordinated to the Fe(III) ion. The appearance of a band at 1480  $\text{cm}^{-1}$  can also be ascribed to the formation of the Fe(Ka-pa)-*n* and Fe(Ka-dpa)-*n* complexes in the basal space of kaolinite. Álvaro et al. have reported the incorporation of Fe(III) picolinate complexes into zeolite Y and Na-mordenite, observing that the presence of the band at 1480  $\text{cm}^{-1}$  can be taken as a spectroscopic evidence for the formation of Fe(pa)<sub>3</sub> complex [4].

Figs. 6 and S3 show the Diffuse-Reflectance UV–vis spectra of the solids Fe(Ka-pa)-3 and Fe(Ka-dpa)-3, compared to the solution spectra of Fe(III) chloride, the ligands pa and dpa, and the complexes Ka-pa and Ka-dpa. The UV–vis spectra of Ka-pa and Ka-dpa display bands at 217 and 265 nm; and 204, 220, and 260 nm, respectively, characteristic of the absorption of picolinic and dipicolinic acids grafted in the inorganic matrix. For the Fe-containing solids, the bands at 196, 220, and 265 nm are associated to ligand to metal charge-transfer (LMCT). These bands can reasonably be attributed to the complexation of Fe(III) species with the ligands grafted on kaolinite [44]. However, other authors [45] consider that these bands are due to the d–d transfer to  $^2E_g$  state. In our solids, this LMCT band seems to be due to the electron transfer from the

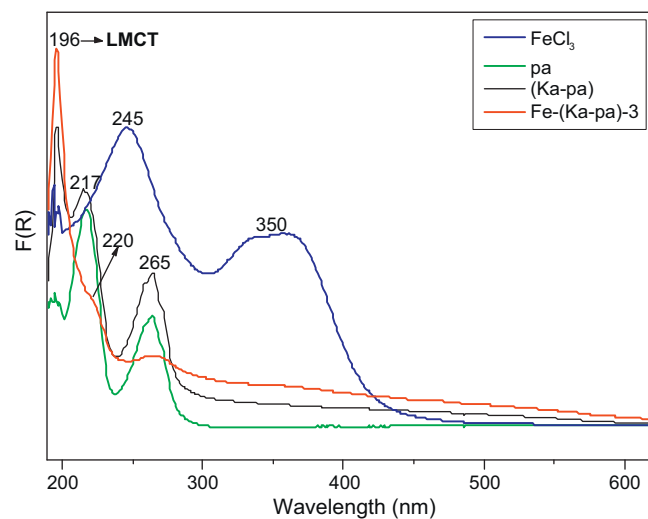


**Fig. 6.** UV/vis spectra of the compounds Fe(III) chloride, picolinic acid (pa), Ka-pa and Fe(Ka-pa)-3.

free electron pair of the nitrogen atoms in pa or dpa anions grafted on kaolinite to the  $t_{2g}$ ,  $E_g$  empty Fe(III) orbitals.

The thermal behavior of the catalysts Fe(Ka-pa)-3 and Fe(Ka-dpa)-3 was investigated by thermogravimetry and differential thermal analysis under oxygen atmosphere (Figs. 7 and S4). Both catalysts showed high thermal stability, above 300 °C. A first mass loss step, with an associated endothermic peak, was observed at 60–65 °C, being attributed to the elimination of small amounts of solvent adsorbed in the clay. Before the intense mass loss ascribed to the thermal decomposition of the complexes, both solids showed a small endothermal effect close to 270 °C, best observed in the DTG curves, probably due to the removal of small amounts of water. The decomposition of the organic ligands appears as a strongly exothermic process, more intense in the Fe(Ka-dpa)-3 solid, centered at 404 °C. This process is actually composed of two steps, centered at 345 and 480 °C in Fe(Ka-pa)-3 solid and at 400 and 498 °C in the case of Fe(Ka-dpa)-3. This may be reasonably ascribed to the removal in the first process of the ligands forming complexes out of the interlayer space and in the second process of the ligands located inside the interlayer space. The fact that the temperature of the second process is considerably higher for the Ka-dpa series may be due to the two carboxylate groups in dpa anions, which makes them to be more strongly bonded to Fe(III) cations. In both cases, the presence

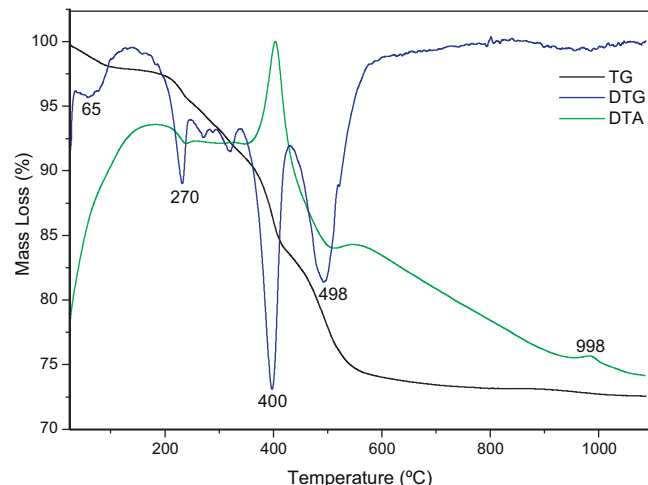


**Fig. 7.** TG/DTA measurements of Fe(Ka-dpa)-3 solid performed in O<sub>2</sub> atmosphere.

**Table 2**  
Thermal analysis results for Ka-pa and Ka-dpa solids.

Sample	Decomposition temperature, °C (Mass loss, %)			
	H <sub>2</sub> O/ethanol	Grafted ligands	Complexed ligands	Kaolinite dehydroxylation
Ka-pa	25–190 (3)	150–380 (24)	–	450–1100 (11)
Fe(Ka-pa)-1	25–190 (3)	200–380 (5)	400–460 (13)	400–1100 (13)
Fe(Ka-pa)-2	25–190 (4)	200–380 (7)	400–600 (13)	400–1100 (18)
Fe(Ka-pa)-3	25–190 (3)	200–380 (15)	400–600 (12)	400–1100 (15)
Ka-dpa	25–200 (3.5)	200–380 (14)	–	400–1100 (16)
Fe(Ka-dpa)-1	25–200 (1)	200–380 (6)	380–420 (7)	400–1100 (12)
Fe(Ka-dpa)-2	25–200 (1)	200–380 (7)	280–420 (8)	400–1100 (11)
Fe(Ka-dpa)-3	25–200 (2)	200–380 (7)	280–420 (8)	400–1100 (11)

of Fe(III) coordinated to the picolinates increases the thermal stability with respect to the corresponding Ka-pa and Ka-dpa precursors, the picolinate anions are eliminated at higher temperatures; in the first case, the pa units decompose at 370 °C and in the second one at 375 and 473 °C [27]. At higher temperatures, the dehydroxylation of kaolinite at 470 °C and the formation of a phase close to mullite at ca. 1000 °C are observed [27,46–49]. The temperature and mass loss in the different processes are summarized in Table 2.

The ligands in the precursors are divided in two types in the final solids, those coordinated or not coordinated to Fe(III) cations. The mass loss corresponding to each type is shown in Table 2. A good agreement is observed between the initial ligand amount and the final values, the small differences may be due to a small leaching of ligands during the incorporation of Fe, and to relative changes in composition due to the variation of the amount of water and of Fe. The amount of ligands is very similar for the solids in each series, but rather different between both series, ca. 13% in Ka-pa series and 8% in dpa series, which is probably related to the higher ligand ability of dpa by the presence of a second carboxylic group. It is noticeable that the amount of coordinated ligands is almost constant in the three solids of a series; this perfectly matches with the fact that the amount of Fe is also almost constant in the three solids, in spite of the different amount added in the synthesis. Thus, the solids in Ka-pa series have Fe contents close to 6.7% and those in Ka-dpa series close to 5.30% (expressed as Fe<sub>2</sub>O<sub>3</sub>, on dry basis and once subtracted the Fe present in the original kaolinite). It is remarkable that the Fe contents are almost constant in each series, as observed in the contents of the ligands. The ratio dpa/Fe results to be close to 2.0, while the ratio pa/Fe is close to 1.0, which seems to be related to the accessibility of Fe(III) to the ligands in the interlayer region.

### 3.2. Oxidation of cis-cyclooctene and cyclohexane by hydrogen peroxide

For various reasons, cis-cyclooctene is often used as a diagnostic substrate whenever a new catalytic system is synthesized. First, the high stability of cis-cyclooctenoxide, its main oxidation product, enables easy evaluation of the catalyst efficiency [50]. Besides, epoxides are very useful intermediates in the chemical industry, since they are the starting point for the preparation of a wide variety of products.

On the other hand, cyclohexane is relatively inert and its oxidation is well reported in the literature, thereby enabling comparison to bibliographic data. This substrate also makes possible the evaluation of the catalyst selectivity because cyclohexanol and/or cyclohexanone can be obtained as oxidation products [50–53]. The industrial importance of the oxidation of cyclohexane is great; as it leads into a mixture of cyclohexanol and cyclohexanone – called K-A oil – employed in the synthesis of textile fibers, such as nylon-6 and nylon-6.6 [51]. This reaction is carried out at industrial level employing soluble Co(II) salts as catalysts, molecular oxygen as

oxidant, and high temperatures (~160 °C) and pressures (15 bar). Under these conditions, conversion levels are as low as 4%, with 80% selectivity to K-A oil and a cyclohexanol/cyclohexanone molar ratio of 2:1 [54]. Although the oxidant used in this system is cheap, it is only efficient at temperatures around 70 °C. Therefore, the search for catalysts that are efficient at mild temperatures is a great challenge for both researchers and industries, as emphasized by Schuchardt et al. [55,56].

The results of the oxidation of cis-cyclooctene catalyzed by Fe(Ka-pa)-*n* and Fe(Ka-dpa)-*n* heterogeneous catalysts and the corresponding homogeneous catalysts Fe(pa)<sub>3</sub> and Fe(dpa)<sub>3</sub> using hydrogen peroxide as oxidant are summarized in Table 3. The conversion was analyzed after 2, 4, 24 and 48 h of reaction. It is remarkable that, in all cases, the selectivity to cyclooctene oxide was 100%.

The heterogeneous catalysts led to high conversions of cis-cyclooctene to cis-cyclooctene epoxide, mainly in the Fe(Ka-pa)-*n* series, in which reached values up to 37%, as indicated with total selectivity to the epoxide. These conversions were similar to those obtained for the corresponding homogeneous system. This clearly suggests that the access to the active Fe(III) sites is easy, lowering the amount of catalyst needed for reaching good conversion values at ambient temperature and pressure. This is an important advantage with respect to some reported biomimetic systems consisting of metalloporphyrins heterogeneized in solid matrices, in which the difficult access of the substrate and the oxidant to the active catalytic sites makes that high oxidant/catalyst ratios have to be used in order to obtain good substrate conversions, also making difficult the reuse of the catalysts.

The lower conversions in the Fe(Ka-dpa)-*n* solids is probably because their lower interlayer heights difficult the access of the substrate to the interlayer region, mainly in the Fe(Ka-dpa)-3 catalyst, which contains the higher amount of organic ligand. The catalysts Fe(Ka-pa)-*n*, in turn, exhibit larger basal distance, allowing a more facile access of the substrate to the catalytic sites in the matrix and explaining the higher yields obtained. Taken together, these data prove that Fe(III) plays a fundamental role in the oxidation reaction. This explanation is reinforced by the amount of complexes present in the basal space of kaolinite, the higher ligand amount in Ka-(pa)<sub>1.59</sub> in relation to Ka-(dpa)<sub>0.38</sub> contributes to the efficiency of the catalyst [26]. The catalysts based on Ka-pa precursor present higher layer disorder than those based on Ka-dpa, which can be assigned to the high amount of picolinic moieties (grafted, intercalated or adsorbed) in the interlayer space of the kaolinite. This higher disorder promotes the accessibility of the substrate to the Fe(III)–picolinate active sites, explaining the higher conversion of Ka-pa solids to cis-cyclooctene (37%) when compared to series Ka-dpa (15%). On the other hand, the longer reaction time necessary for substrate conversion in the case of the heterogeneized catalysts is expectable considering the morphology of the kaolinite matrix, which may hinder the access of the reagents to the active catalytic sites. In any case, it can be said that the performance



**Table 3**  
Conversion of cis-cyclooctene to cyclooctenoxide catalyzed by Ka-pa and ka-dpa-containing systems.<sup>a</sup>

Catalyst	2 h (%)	TON	4 h (%)	TON	24 h (%)	TON	48 h (%)	TON
Ka-pa	–	–	–	–	–	–	–	–
Fe(pa) <sub>3</sub>	7.0	2349	7.0	2349	25.0	8391	36.0	12083
Fe(Ka-pa)-1	4.0	134	5.0	168	22.0	741	29.0	977
Fe(Ka-pa)-2	4.0	134	4.0	134	22.0	741	34.0	1141
Fe(Ka-pa)-3	7.0	234	10.0	335	35.0	1174	37.0	1241
Ka-dpa	–	–	–	–	–	–	–	–
Fe(dpa) <sub>3</sub>	4.0	914	4.0	914	7.0	1600	11.0	2515
Fe(Ka-dpa)-1	4.0	69	4.0	69	9.0	157	12.0	209
Fe(Ka-dpa)-2	4.0	69	4.0	69	9.0	157	14.0	243
Fe(Ka-dpa)-3	4.0	69	4.0	69	9.0	157	15.0	342

<sup>a</sup> Conditions: molar ratio of catalyst/oxidant/cis-cyclooctene was 1:300:100; solvent mixture acetonitrile/dichloroethane (ACN/DCE, 1:1, v/v). Homogeneous catalysts Fe(pa)<sub>3</sub> and Fe(dpa)<sub>3</sub> were obtained under the same conditions as the heterogeneous catalysts. All the reactions were conducted at 25 °C and ambient pressure. Turnover Number (TON) = sum of products conversion (mol)/amount of “active component” (mol).

of the Fe(III)–picolinate grafted catalysts is good. It can again be remarked that all the reactions involved herein proceed by a typical heterogeneous catalysis mechanism, since Fe–picolinate and dipicolinate complexes did not leach from the support during the entire process.

The consumption of hydrogen peroxide was investigated after the catalysis oxidation reactions. For all reactions, when Fe(Ka-pa)-*n* and Fe(Ka-dpa)-*n* were employed as heterogeneous catalysts the hydrogen peroxide was fully consumed during the reaction, this gives good evidences that the Fe(III) picolinate and dipicolinate grafted on kaolinite are able to transfer the oxygen to the substrate with high efficiency. The catalysts were successfully reused in the oxidation reaction using hydrogen peroxide as oxidant. The catalysts were separated from the reaction mixture after each experiment by simple filtration, washed and dried before being used in the subsequent runs. Good conversions were maintained for the first five reuses.

As for cyclohexane oxidation, all heterogeneous catalysts based on Ka-dpa precursor were more selective for cyclohexanone formation compared to the homogeneous reaction, however all the catalysts based on Ka-pa present low selectivity for ketone or alcohol. This fact can be explained by the morphology of these solids, the easy accessibility to their active sites promote the fast oxidation of cyclohexane and the diffusion of this product to the reaction medium. But in the specific case of solids based on Ka-dpa the difficult accessibility and release of products from the active sites promote the higher selectivity to the ketone, the cyclohexanol obtained is reoxidized by hydrogen peroxide and only ketone is released from Fe-(Ka-dpa)-*n* matrix, as seen from the results presented in Table 4.

In particular, the catalysts Fe(Ka-dpa)-1, Fe(Ka-dpa)-2, and Fe(Ka-dpa)-3 were the most selective for cyclohexanone formation, furnishing ketone yields of 5, 5, and 7% after 48 h, respectively (ambient temperature and pressure). The formation of cyclohexanone in higher proportion can be explained by the amount of complex present in the basal space of the clay, which must resemble the surroundings of the metal ion in the biomimetic Fe model, thereby giving rise to site-isolation in the case of the grafted complexes. In the specific case of Fe(Ka-dpa)-*n*, the basal space of the catalysts is smaller (11.4 Å), not to mention the existence of phases with basal distances of 8.4, 6.3 and 5.5 Å, assigned to the presence of “halloysite-like” structures with internal diameter of 30 nm. These tubular phases with shorter basal distance are probably the reason for the higher selectivity of these catalysts. The difficult release of products from the active catalytic sites certainly causes further oxidation of the initially formed cyclohexanol to cyclohexanone. It is important to bear in mind that the empty spaces inside the kaolinite nanotubes are occupied by hydrophobic organic molecules, as picolinate, carrying complexes displaying catalytic activity, and the restricted movement and diffusion of

the substrate (cyclohexane) favors its oxidation (to cyclohexanol) and re-oxidation (to cyclohexanone), as previously reported by Nakagaki et al. for ironporphyrins immobilized on silylated halloysite nanotubes [37–39]. It is generally expected that ironporphyrins functioning as biomimetic models of cytochrome P-450 should lead to higher yields of cyclohexanol than of cyclohexanone. In fact, high selectivity for the alcohol product has been observed by several authors. However, the fact that Fe(III)–dipicolinate immobilized on kaolinite was more selective for cyclohexanone (100%) shows that these materials grafted on kaolinite outperformed the catalysts currently employed by the industry, not to mention that all the reactions carried out here were accomplished in mild conditions (ambient temperature and pressure, environmentally friendly oxidant). Experiments conducted under similar conditions, but in the absence of catalysts and with materials that were not complexed with Fe(III), namely Ka-pa and Ka-dpa, did not give any oxidation products, proving that Fe(III) plays a crucial role in the catalytic oxidation reactions [57–59].

The selectivity achieved with the catalysts Fe(Ka-dpa)-*n* is higher than those reported by Esmelindro et al. [19], who used a binuclear iron complex as catalyst in the oxidation of cyclohexane by hydrogen peroxide. These authors observed a conversion of 19% of cyclohexane, but the selectivity cyclohexanol/cyclohexanone was close to 2:1 (12.65% of cyclohexanol and 6.59% of cyclohexanone). In this homogeneous system, the binuclear Fe(III) complex acted as methanemoneoxygenase model, with high selectivity for the alcohol. However, no data on the reuse of the catalyst were reported for this system [60]. Again in this case, the reaction was entirely heterogeneous; no leaching of Fe–picolinate and dipicolinate complexes was observed.

Our present results in the oxidation of cis-cyclooctene and cyclohexane demonstrate the catalytic potential of iron complexes supported on clays, mainly regarding the high selectivity toward cyclohexanone. These data are even more interesting given that selectivity for cyclohexanol is usually found, as in the case of the industrial process for production of adipic acid and  $\epsilon$ -caprolactam. Moreover, the Fe–picolinate–clay system is advantageous because it is heterogeneous, much cheaper than other systems, the catalysts are synthesized in mild conditions – low temperature and ambient pressure – and they are active in catalytic oxidation reactions using an eco-friendly oxidant as H<sub>2</sub>O<sub>2</sub>.

With the aim of investigating the influence of temperature in the catalytic oxidation and of optimizing this process, the best catalysts (Fe(Ka-pa)-3 and Fe(Ka-dpa)-3) were employed in both oxidation reactions at 55 °C, as it has been reported that in some cases higher temperatures facilitate the diffusion of the substrate to the active catalytic sites, thereby enhancing conversion of the reactants. The catalyst/oxidant/substrate molar ratio was maintained at 1:300:100, the same used at ambient temperature.

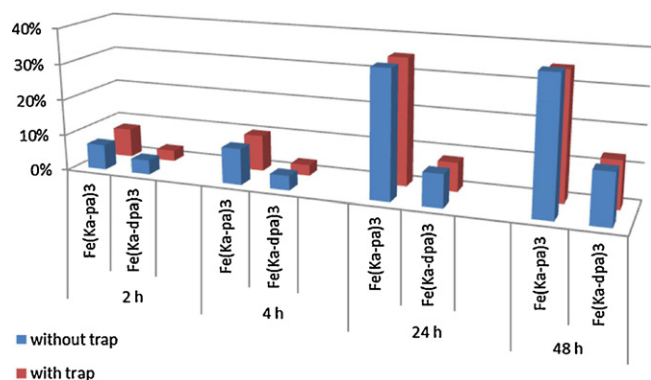


Fig. 8. Effect of hydroquinone on conversion of cis-cyclooctene to cyclooctenoxide.

In the case of Fe(Ka-pa)-3, its activity at 55 °C was lower than at RT, probably due to a partial leaching of Fe(III)-picolinate from the interlayer space of the clay. According to Shul'pin et al., simple salts have lower activity than complexes, and in the case of homogeneous catalysis the activity of the complexes is much lower compared to that of the supported catalysts [57]. On the other hand, in presence of hydrogen peroxide, the higher temperature might provoke the decomposition of the complexes immobilized in the interlayer space of kaolinite. However, in the case of Fe(Ka-dpa)-3, the increase of the reaction temperature to 55 °C promoted higher substrate conversion. The fact that dipicolinate anion has two carboxylic groups gives rise to a more stable material than in the case of the picolinate, as these groups are covalently bound to the clay via two hydroxyl groups, what justifies a lower leaching degree. Specifically for the case of cyclohexane oxidation, the results prove that the higher temperature enhances the diffusion of the substrate, thereby increasing cyclohexanone yields (14%). The higher selectivity for cyclohexanone (100%) compared to reactions conducted at ambient temperature was attributed to the presence in this catalyst of a tubular phase of kaolinite (halloysite-like), as confirmed by XRD and TEM analyses.

To study the mechanisms involved in the formation of the products during cis-cyclooctene and cyclohexane oxidation, all the catalysts were studied again in similar conditions, but in the presence of the radical scavenger hydroquinone. Fig. 8 displays the conversion observed for cis-cyclooctene oxidation reaction in the presence of this radical scavenger. These data strongly suggest that a nonradical pathway is responsible for the selective oxidation reaction. In fact, the presence of radical active species was ruled out for both substrates, which was corroborated by the absence of byproducts like cyclohexylhydroperoxide. The oxidation is thus probably performed via a non-radical mechanism involving high-valent Fe-oxo species.

The efficiency and stability of Fe-picolinate-clay system was analyzed by evaluation of its reuse. For this purpose, the solid catalysts were separated from the reaction mixture after each experiment by simple filtration and dried before being used in a subsequent run. In the case of the samples Fe-(Ka-pa)-*n* and Fe(Ka-dpa)-*n*, the catalysts were reused in five consecutive runs without any decrease in activity. On the other hand, to determine if catalysis is genuinely heterogeneous the catalysts Fe(Ka-pa)-*n* and Fe(Ka-dpa)-*n* were filtered off the reaction mixture after a catalytic cycle, an extra amount of oxidant was added to the resulting supernatant, and the oxidation reaction was allowed to proceed under the same initial conditions for 72 h. After this period, no cis-cyclooctene oxide yields were detected, indicating that the catalytic activity of the solid catalysts is truly heterogeneous and also demonstrating that the Fe(III)-pyridine carboxylic complexes play an essential role in the catalysis.

Table 4  
Conversion (%) of cyclohexane to cyclohexanol (OL) and cyclohexanone (ONE) using the indicated catalysts and after different reactions times.<sup>a</sup>

Catalysts	2 h			4 h			24 h			48 h		
	OL	ONE	TON	OL	ONE	TON	OL	ONE	TON	OL	ONE	TON
Ka-pa	-	-	-	-	-	-	-	-	-	-	-	-
Fe(pa) <sub>3</sub>	3.0	3.5	2181	4.0	5.0	3021	8.0	10.0	6042	7.0	7.0	4699
Fe(Ka-pa)-1	2.0	1.7	124	2.0	2.0	134	3.0	4.0	236	5.0	6.0	370
Fe(Ka-pa)-2	0.5	1.0	51	1.0	2.0	102	3.0	2.5	185	1.0	2.0	101
Fe(Ka-pa)-3	2.0	1.0	102	2.0	1.5	118	2.0	3.0	168	2.0	3.5	185
Ka-dpa	-	-	-	-	-	-	-	-	-	-	-	-
Fe(dpa) <sub>3</sub>	-	-	-	-	-	-	3.0	2.0	1143	3.0	4.0	1600
Fe(Ka-dpa)-1	-	-	-	-	-	-	-	4.0	88	-	7.0	155
Fe(Ka-dpa)-2	-	-	-	-	-	-	-	3.0	66	-	5.0	110
Fe(Ka-dpa)-3	-	-	-	-	1.0	22	-	3.0	66	-	5.0	110

<sup>a</sup> Conditions: the same as in Table 3.

**Table 5**  
Cyclohexane oxidation by PhIO using the indicated catalysts and after different reactions times.<sup>a</sup>

Catalysts	2 h		4 h		24 h		48 h	
	OL	ONE	OL	ONE	OL	ONE	OL	ONE
Ka-pa	–	–	–	–	–	–	–	–
Fe(Ka-pa)-3	–	16.0	–	14.5	–	16.0	–	17.0
Ka-dpa	–	–	–	–	–	–	–	–
Fe(Ka-dpa)-3	–	10.0	–	9.5	–	10.0	–	11.0

<sup>a</sup> Conditions: catalyst/oxidant/cyclohexane = 10 mg catalyst, 5 mg PhIO, 150  $\mu$ L cyclohexane; solvent mixture acetonitrile/dichloroethane (ACN/DCE, 1:1, v/v). All the reactions were conducted at 25 °C and ambient pressure. % = product yield.

The activity of heterogeneous catalysis is kinetically controlled by two principal factors, *i.e.*, the number of active sites on catalyst surface and the turnover number (TON) of reaction on each active site. Homogeneous catalysts generally have high turnover numbers due the easiness of diffusion of substrate and products, while solid catalysts suffer some irreversible chemical changes in their surfaces affecting the reaction mechanism and the diffusion and access to active sites. Thus, picolinate and dipicolinate complexes in homogeneous medium shows high TON values (see Tables 3, 4 and 7), while the lower TON in heterogeneous catalysts can be explained due to the difficult access to active sites located in the interlayer space of kaolinite. However, it may be emphasized that these heterogeneous catalysts based on kaolinite can be easily reutilized by several times with constant catalytic activity.

### 3.3. Oxidation of *cis*-cyclooctene and cyclohexane by PhIO

Iodosylbenzene has various interesting peculiarities as oxidant: it gives good oxidant conversion; it is relatively inert in the absence of iron complexes, forming with them high-valent ferryl radicals  $\text{Fe}^{\text{IV}}(\text{O})^+$  and PhI; it is a polymeric solid that does not contain weak O–H bonds, thus eliminating the occurrence of free radical chain reactions normally initiated by oxidants such as alkyl hydroperoxides, R–O–O–H [60]. By these reasons, the oxidation of *cis*-cyclooctene, cyclohexane, and cyclohexanol with this oxygen source was investigated, catalyzed by the precursors Ka-pa and Ka-dpa and the catalysts Fe(Ka-pa)-3 and Fe(Ka-dpa)-3.

The oxidation of *cis*-cyclooctene was in all cases null when using the precursors, even when the reaction was carried out for 48 h, and in spite of the small amount of Fe in the parent kaolinite. In opposite, the Fe-containing solids Fe(Ka-pa)-3 and Fe(Ka-dpa)-3 catalyzed quantitatively the reaction in all the conditions considered, even after only 2 h of reaction. It is noteworthy that the heterogeneous systems furnished higher yields compared to the parent heterogeneous catalysts (without iron). The fact that the conversion is very high from short reaction times is a very promising result, since one of the usual disadvantages of heterogeneous catalysts is the fact that they require long reaction times, because the matrix hinders the access of the substrate to the active catalytic sites and slows down the diffusion of the products. Active sites in our grafted kaolinite seem to be easily available, probably because of the layered structure and relatively high interlayer height of both catalytic systems.

It is important to highlight that catalysts based on the Ka-dpa precursor gave lower product yields compared to the catalysts based on Ka-pa. This may be justified by the more difficult access of the reactants to the active sites in the former materials, and by the smaller quantity of Fe(III) complex immobilized in their interlayer space. Indeed, Fe-(Ka-pa)-*n* and Fe(Ka-dpa)-*n* catalysts show distinct morphologies. In the particular case of Ka-dpa, the materials obtained after complexation with Fe(III) in aqueous media presented tubular morphology; the tubular nature of the Fe(Ka-dpa)-*n* catalysts might contribute to their selectivity, once the

functionalized part of the clay faces the interior part of the formed tubes, thus the active sites are more protected and the access of the substrate and the oxidant to these sites more restricted, thereby becoming a limiting factor for their reactivity.

The results obtained for the oxidation of cyclohexane are shown in Table 5. The precursors Ka-pa and Ka-dpa were again not active for this reaction, and the Fe-containing solids showed relatively high cyclohexane conversions, between 9.5 and 17.0%. Various aspects may be remarked in these results. First of all, it is very significant that selectivity was complete for cyclohexanone for both catalysts, cyclohexanol was not detected. Also in both cases, the conversion is almost constant with time; in fact, high conversions are observed for the shorter time considered (2 h), slightly decreasing after 4 h (confirming the tendency observed in the oxidation of cyclooctene), increasing a little for higher reaction times. This again confirms that the catalytically active sites are easily accessible to the reactant and the oxidant. Finally, conversion is again significantly higher when using Fe(Ka-pa)-3 catalysts than when using Fe(Ka-dpa)-3.

Cyclohexanone can be formed in a single step, by direct oxidation of cyclohexane, or in two steps, by the oxidation of cyclohexanol previously formed by oxidation of cyclohexane. Trying to gain information on the catalytic activity of the solids, cyclohexanol was used as substrate, being oxidized under the same conditions. The results obtained are shown in Table 6. Both Fe(Ka-pa)-3 and Fe(Ka-dpa)-3 catalysts are really able to oxidize cyclohexanol to cyclohexanone. However, in the case of the matrix based on the Ka-pa precursor, with much larger basal spacing, cyclohexanol does not remain in contact with the active site for long, being rapidly released into solution, while for the Ka-dpa series solids, the kaolinite tubes present in their structure make cyclohexanol diffusion to the solution slower, allowing the oxidation of the alcohol to the ketone. This is more clearly evident when reactions using  $\text{H}_2\text{O}_2$  as oxidants are analyzed; cyclohexanol and cyclohexanone are formed. Nevertheless, catalysts based on the Ka-dpa precursor give selectivities of up to 87% for cyclohexanone when the reaction is performed at 60 °C, and 100% selectivity is achieved in the reactions carried out at ambient temperature and using PhIO and/or  $\text{H}_2\text{O}_2$ . No conversion was observed when the solids Ka-pa and Ka-dpa were employed in the same conditions.

It has been reported that the addition of aminoacids to catalytic systems composed of metal catalysts considerably increases

**Table 6**  
Oxidation of cyclohexanol to cyclohexanone by PhIO catalyzed by using the indicated catalysts and after different reactions times.<sup>a</sup>

Catalysts	2 h	4 h	24 h	48 h
Ka-pa	–	–	–	–
Fe(Ka-pa)-3	17.0	48.0	90.0	100
Ka-dpa	–	–	–	–
Fe(Ka-dpa)-3	16.0	18.0	75.0	75.0

<sup>a</sup> Conditions: the same as in Table 5.

alkane conversion in the case of cyclohexane oxidation by H<sub>2</sub>O<sub>2</sub>, the aminoacids seem to play the role of co-catalysts. In our system, the picolinic acids seem to play a similar role, which can be attributed to the fact that their structure, because of the vicinity between the amino and the acid groups, is in a certain way similar to that of the aminoacids.

Shul'pin et al. [57] described that the catalytic activity of a dinuclear iron complex in the oxidation of cyclohexane was improved by using H<sub>2</sub>O<sub>2</sub> as oxidant, while according to Nizova et al. [61], this oxidation occurs by a radical mechanism that involves initial reduction of a Fe(III) cation by H<sub>2</sub>O<sub>2</sub> and consequent formation of hydroperoxy radicals and Fe(II); the role of the aminoacid is to facilitate the proton transfer between the coordinated H<sub>2</sub>O<sub>2</sub> and the iron ion, thereby producing the Fe–O–OH fragments [62]. In our catalytic system, the use of a radical trap (hydroquinone) did not modify the results, suggesting the occurrence of a non-radical mechanism of oxidation. However, when triphenylphosphine (PPh<sub>3</sub>) was added to the reaction medium, the conversion of cyclohexanol to cyclohexanone was higher (Table 7). In the case of a radical mechanism, formation of both cyclohexanol and cyclohexanone increases after addition of PPh<sub>3</sub>. This has been reported to occur in the GC injector through transformation of alkyl hydroperoxides, which are reduced by PPh<sub>3</sub>, to give the alcohol [62].

On the basis of the results obtained with hydroquinone and PPh<sub>3</sub> a mechanism for the catalytic activity of Fe-picolinate-kaolinite catalysts can be proposed (Fig. 9). This mechanism is similar to that reported by Gozzo [62], who detected the reduction of the Fe(III)–pyridine carboxylate complex to the corresponding Fe(II)–pyridine carboxylate complex in the presence of excess H<sub>2</sub>O<sub>2</sub>. These authors reported that the Fe(II) complex subsequently reacted with H<sub>2</sub>O<sub>2</sub> and, in the presence of pyridine from the amino acid residue, a non-radical mechanism then took place. In this non-radical mechanism, the active species responsible for oxygen transfer to the substrate is HO–Fe<sup>IV</sup>–O–OH, which leads to the formation of alkyl hydroperoxide, the latter of which produces cyclohexanol. In the presence of PPh<sub>3</sub>, the hydroperoxide is reduced to the alcohol, which accounts for the occurrence of the non-radical mechanism, as previously discussed by Gozzo in the case of the GIF-catalysts mechanism involving Fe(II)–bispicolinate complexes [62]. Pyridine derivatives are believed to be essential for the system as a trap for hydroxyl radical, thereby preventing Fenton chemistry.

#### 3.4. Baeyer–Villiger oxidation reaction of cyclohexanone

Table 8 displays the results from the Baeyer–Villiger reaction carried out for oxidation of cyclohexanone to  $\xi$ -caprolactone, using Fe(Ka-pa)-3 and/or Fe(Ka-dpa)-3 as catalysts. The reaction was carried out under various different conditions, and the following conclusions are found:

- Presence of benzonitrile: it is necessary for the reaction, in the absence of this solvent, there was no  $\xi$ -caprolactone formation. This effect has already been observed previously, and it is proposed that benzonitrile participates in the transference of oxygen [6,34–38,63].
- Temperature: it is a decisive factor. When the reactions were conducted at ambient temperature, the conversions were lower than 2% after 24 h of reaction while, as observed in Table 8, much higher conversions are obtained when the reaction is carried out at 60 °C.
- Conversions of 45 and 60% were obtained after 24 h of reaction. The selectivity was complete for  $\xi$ -caprolactone, no other products were detected.
- Presence of Fe(III) complexes: they are the true catalysts, when the reaction was carried out in the absence of any catalyst, or in

**Table 7**  
Cyclohexane oxidation by 70 wt.% H<sub>2</sub>O<sub>2</sub> after 48 h, with addition of excess PPh<sub>3</sub>, at two different temperatures.<sup>a</sup>

Catalyst/temperature	2 h			4 h			24 h			48 h			48 h × PPh <sub>3</sub>		
	OL	ONE	TON	OL	ONE	TON	OL	ONE	TON	OL	ONE	TON	OL	ONE	TON
Ka-pa	–	–	–	–	–	–	–	–	–	–	–	–	–	–	–
Fe(Ka-pa)-3/25 °C	–	2.0	67	–	2.5	84	–	6.0	202	–	4.0	4.0	0.3	1.5	61
Fe(Ka-pa)-3/55 °C	3.0	4.0	236	7.0	8.0	505	11.0	8.0	640	11.0	8.0	19.0	13.0	10.0	775
Ka-dpa	–	–	–	–	–	–	–	–	–	–	–	–	–	–	–
Fe-(Ka-dpa)-3/25 °C	–	1.0	22	–	1.0	22	–	3.0	66	–	6.0	6.0	6.0	5.0	243
Fe-(Ka-dpa)-3/55 °C	2.0	3.0	110	5.0	5.0	221	7.0	10.0	376	8.0	11.0	19.0	10.0	12.0	487

<sup>a</sup> Conditions: catalyst/oxidant/cyclohexane molar ratio = 1:300:100; solvent mixture acetonitrile/dichloroethane, (ACN/DCE, 1:1, v/v); ambient pressure. Turnover Number (TON) = sum of products conversion (mol)/amount of "active component" (mol).



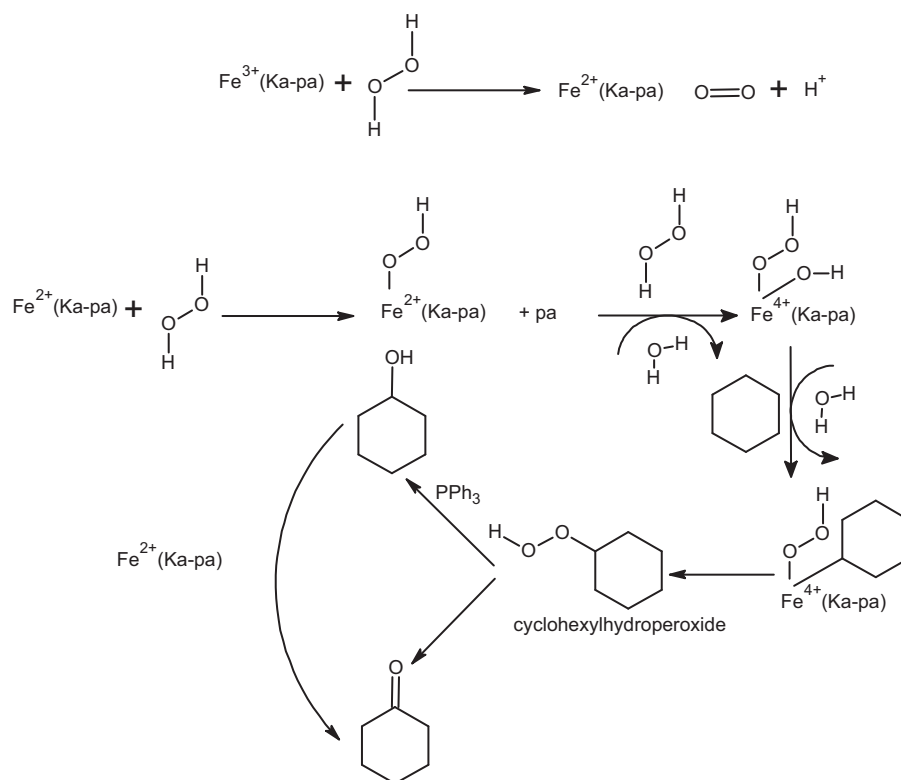


Fig. 9. Possible mechanism for the oxidation of cyclohexane (Adapted from Gozzo mechanism for GIF-catalysts).

the presence of the solids non-containing iron, Ka-pa and Ka-dpa, very low substrate conversions were observed (less than 1%).

The reaction was carried out using two different hydrogen peroxide concentrations (30 and 70 wt.%), this implies different amounts of water in the reaction medium. For both catalysts, the best results were achieved with 70 wt.%  $\text{H}_2\text{O}_2$ . In some cases, the presence of water can deactivate a catalyst, since water molecules can coordinate to its active sites. In this sense, further investigations of the hydrophilicity of Fe-picolinate-kaolinite system are necessary, because this is an essential parameter when  $\text{H}_2\text{O}_2$  is employed in aqueous medium. Steffen et al. [64], studying the Baeyer–Villiger reaction catalyzed by commercial alumina or alumina prepared by the sol–gel process, have reported that the reactions accomplished with  $\text{H}_2\text{O}_2$  in anhydrous medium furnished higher yields compared

to those carried out in aqueous medium [24,34–38]. The layered structure of the support resulted in good maintenance of its properties. Even under various catalytic cycles, problems related to the diffusion of the reactants to the iron–picolinate complexes, active sites or of the products out of the catalyst were not observed, in contrast with what is observed for other supports, such as silica and alumina.

It has been proposed that the Baeyer–Villiger reaction consists of two steps: the first one comprises a nucleophilic attack on the carbonyl, with formation of the Criegee adduct, and the second one involves a concerted rearrangement of the intermediate, thereby generating an ester and a carboxylic acid [6,63]. Water is formed as byproduct when  $\text{H}_2\text{O}_2$  is employed as oxidant, while a carboxylic acid is formed if using a peracid as oxidant. A detailed mechanism for the Baeyer–Villiger oxidation catalyzed by

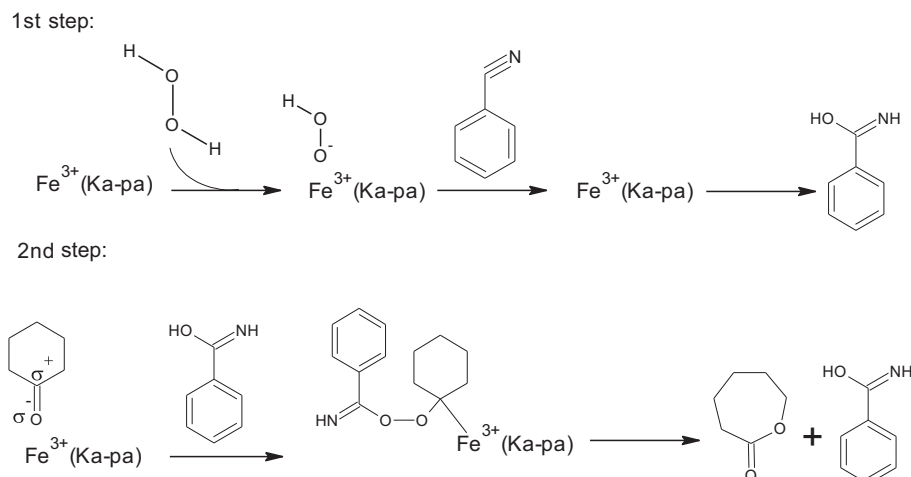


Fig. 10. Possible mechanism for the Baeyer–Villiger oxidation in the presence of benzonitrile (Adapted from Ruiz [6]).

**Table 8**  
Amount of  $\xi$ -caprolactone obtained (%) by Baeyer–Villiger oxidation of cyclohexanone by 30 and 60 wt.%  $H_2O_2$  using the indicated catalysts.<sup>a</sup>

Catalyst	Oxidant					
	2 h		4 h		24 h	
	30% $H_2O_2$	60% $H_2O_2$	30% $H_2O_2$	60% $H_2O_2$	30% $H_2O_2$	60% $H_2O_2$
Ka-pa	–	–	–	–	–	–
Fe(pa) <sub>3</sub>	38.0	55.0	59.0	65.0	68.0	79.0
Fe(Ka-pa)-3	21.0	38.0	27.0	43.0	33.0	60.0
Fe(Ka-pa)-3 A.T. <sup>b</sup>	–	–	–	–	–	–
Fe(Ka-pa)-3 WBz <sup>c</sup>	–	–	–	–	–	–
Ka-dpa	–	–	–	–	–	–
Fe(dpa) <sub>3</sub>	22.0	33.0	28.0	53.0	40.0	68.0
Fe(Ka-dpa)-3	12.0	31.0	14.0	39.0	24.0	45.0
Fe(Ka-dpa)-3 A.T. <sup>b</sup>	–	–	–	–	–	–
Fe(Ka-dpa)-3 WBz <sup>c</sup>	–	–	–	–	–	–

<sup>a</sup> Conditions: catalyst/oxidant/cyclohexane = 20 mg catalyst, 176  $\mu$ L  $H_2O_2$ , 850  $\mu$ L benzonitrile, acetonitrile:dichloroethane: ACN/DCE (1:1, v/v). All the reactions were conducted at 60 °C and ambient pressure. The stoichiometric ratio (number of moles) of peroxide was maintained; only the concentration of water in the system was varied.

<sup>b</sup> Reactions were conducted at ambient temperature and pressure.

<sup>c</sup> Reactions were conducted without benzonitrile, which was substituted by a mixture ACN/DCE (1:1, v/v).

iron-picolinate-kaolinite catalysts is proposed in Fig. 10. In the case of the electrophilic activation of the substrate, the acid sites in iron-picolinate-kaolinite catalysts, as well as electron withdrawing substituents, are able to activate the carbonyl group in cyclohexanone, thereby enhancing the polarizability of the C=O double bond, which in turn facilitates the nucleophilic attack of  $H_2O_2$ . The peroxide thus bonded to Fe cations is able to oxidize benzonitrile to peroxy-carboximidic acid intermediate, which in turn can interact with cyclohexanone forming the Criegee adduct and allowing the oxidation to caprolactone. In this sense, one of the factors that make a catalyst efficient for the Baeyer–Villiger reaction is its ability to increase the nucleophilicity of the peroxide, this activation promotes higher affinity of the oxidant for electron deficient centers [24,34–38], as is the case of the carbonyl group immobilized by its interaction with the picolinate-kaolinite system.

#### 4. Conclusions

Kaolinite covalently grafted with picolinate and dipicolinate anions proved to be viable supports for the effective immobilization of iron by forming complexes. The catalytic results obtained for the complexes covalently grafted into the basal space of kaolinite demonstrated that these catalysts perform well in cis-cyclooctene and cyclohexane oxidation, their activities are similar to those displayed by the corresponding homogeneous complexes. In the case of cyclohexane oxidation, the catalysts Fe(Ka-dpa)-*n* are efficient and highly selective, which is attributed to the presence of a kaolinite tubular phase. Compared to the parent homogeneous catalysts, the heterogeneous catalysts were advantageous with respect to cis-cyclooctene and cyclohexane oxidation reactions since they allowed for the use of mild conditions (temperature and ambient pressure, use of non-polluting oxidants) and promoted high activity and product selectivity. The main advantage of the kaolinite grafted complexes is their easy separation from the reaction mixture by simple filtration of the solid, thus enabling catalyst reuse.

#### Acknowledgments

Spanish authors thank financial support from Spanish Ministry of Science and Innovation (MICINN) and the European Regional Development Fund (FEDER) through projects MAT2010-21177-C02, and Junta de Castilla y León (SA009A11-2). The Brazilian group thanks support from Brazilian Research funding agencies FAPESP and CNPq, and Peróxidos do Brasil (Solvay) for supplying the 70 wt.% aqueous hydrogen peroxide solution.

#### Appendix A. Supplementary data

Supplementary data associated with this article can be found, in the online version, at doi:10.1016/j.cattod.2011.11.029.

#### References

- [1] Ullmann's Encyclopedia of Industrial Chemistry, 7th edition, Wiley-VCH Verlag, Weinheim, 2005.
- [2] G. Centi, S. Peranthoner, *Microporous Mesoporous Mater.* 107 (2008) 3–15.
- [3] Z.L. Lu, E. Lindner, H.A. Mayer, *Chem. Rev.* 102 (2002) 3543–3578.
- [4] M. Álvaro, B. Ferrer, H. Garcia, A. Sanjuán, *Tetrahedron* 55 (1999) 11895–11902.
- [5] R.D. Dewhurst, A.F. Hill, M.K. Smith, *Angew. Chem. Int. Ed.* 43 (2004) 476–478.
- [6] J.R. Ruiz, C. Jiménez-Sanchidrián, R. Llamas, *Tetrahedron* 62 (2007) 11697–11703.
- [7] R.A. Reziq, D. Avnir, I. Miloslavski, H. Schumann, J. Blum, *J. Mol. Catal. A: Chem.* 185 (2002) 179–185.
- [8] A.P.M. Wight, E. Davis, *Chem. Rev.* 102 (2002) 3589–3614.
- [9] Z.L. Lu, E. Lindner, H. Mayer, *Chem. Rev.* 102 (2002) 3543–3578.
- [10] A. Godelitsas, D. Charistos, C. Tsipis, P. Misaelides, A. Filippidis, M. Schindler, *Microporous Mesoporous Mater.* 61 (2003) 69–77.
- [11] M. Hartmann, L. Kevan, *Chem. Rev.* 99 (1999) 635–663.
- [12] R. Bechara, D. Balloy, J. Dauphin, J. Grimblot, *Chem. Mater.* 11 (1999) 1703–1711.
- [13] J.M. Thomas, R. Raja, *Catal. Today* 117 (2006) 22–31.
- [14] L.R.D. da Silva, L.C. Garla, *Quim. Nova* 2 (1998) 169–174.
- [15] A.N. Pour, Y. Zamani, A. Tavasoli, S.M.K. Shahri, S.A. Taheri, *Fuel* 87 (2008) 2004–2012.
- [16] V.H. Deshpande, D.E. Ponde, V.J. Bulbule, A. Sudalai, A.S. Gajare, *J. Org. Chem.* 63 (1998) 1058–1063.
- [17] S. Letáief, B. Casal, P. Aranda, M.A. Martín-Luengo, E. Ruiz-Hitzky, *Appl. Clay Sci.* 22 (2003) 263–277.
- [18] S. Nakagaki, F.L. Benedito, F. Wypych, *J. Mol. Catal. A: Chem.* 217 (2004) 121–131.
- [19] O.A.C. Antunes, M.C. Esmelindro, E.G. Oestreicher, H. Marquéz-Alvarez, C. Dariva, S.M.S. Egues, C. Fernandes, A.J. Bortoluzzi, V. Drago, *J. Inorg. Biochem.* 99 (2005) 2054–2061.
- [20] K.C. Gupta, A.K. Sutar, *Coord. Chem. Rev.* 252 (2008) 1420–1450.
- [21] J.E. Gardolinsky, G. Lagaly, *Clay Miner.* 40 (2005) 547–566.
- [22] J. Murakami, T. Itagaki, K. Kuroda, *Solid State Ionics* 172 (2004) 279–282.
- [23] P.T. Anastas, M.M. Kirchoff, T.C.A. Williamsom, *Catalysis A* 221 (2001) 3–13.
- [24] R.L. Frost, J. Kristof, E. Horvat, J.T. Klopogge, *Spectrochim. Acta. A* 56 (2000) 1191–1204.
- [25] N. Bizaia, E.H. de Faria, G.P. Ricci, P.S. Calefi, E.J. Nassar, K.A.D.F. Castro, S. Nakagaki, K.J. Ciuffi, R. Trujillano, M.A. Vicente, A. Gil, S.A. Korili, *Appl. Mater. Interface* 11 (2009) 2667–2678.
- [26] P. Gómez-Romero, C. Sanchez, *New J. Chem.* 29 (2005) 57–58.
- [27] E.H. de Faria, O.J. Lima, K.J. Ciuffi, E.J. Nassar, M.A. Vicente, R. Trujillano, P.S. Calefi, *J. Colloid Interface Sci.* 335 (2009) 210–215.
- [28] L.R. Ávila, E.H. de Faria, K.J. Ciuffi, E.J. Nassar, P.S. Calefi, M.A. Vicente, R. Trujillano, *J. Colloid Interface Sci.* 341 (2010) 186–193.
- [29] E.H. de Faria, K.J. Ciuffi, E.J. Nassar, M.A. Vicente, R. Trujillano, P.S. Calefi, *Appl. Clay Sci.* 48 (2010) 516–521.
- [30] S.L. Jain, P. Bhattacharyya, *Inorg. Chim. Acta* 359 (2006) 4398–4402.
- [31] A. Goti, F. Cardona, *Green Chem. React.* (2008) 191–212.
- [32] S. Nakagaki, F. Wypych, *J. Colloid Interface Sci.* 315 (2007) 142–157.

- [33] S. Nakagaki, G.S. Machado, M. Halma, A.A.S. Marangon, K.A.D.F. Castro, N. Matoso, F. Wypych, *J. Catal.* 242 (2006) 110–117.
- [34] K. Weissmehl, H.-J. Arpe, (C.R. Lindley, Trans.), *Industrial Organic Chemistry*, vol. 237, 3rd ed., VCH Publishers, Weinheim, 1997.
- [35] G.-J. ten Brink, I.W.C.E. Arends, R.A. Sheldon, *Chem. Rev.* 104 (2004) 4105–4123.
- [36] Z. Lei, G. Ma, C. Jia, *Catal. Commun.* 8 (2007) 305–309.
- [37] Z. Lei, L. Wei, R. Wang, G. Ma, *Catal. Commun.* 9 (2008) 2467–2469.
- [38] S.E. Jacobson, R. Tang, F.J. Mares, *Chem. Commun.* 12 (1978) 888–889.
- [39] V. Amani, N. Safari, H.R. Khavasi, P. Mirzei, *Polyhedron* 26 (2007) 4908–4914.
- [40] J.G. Sharefkin, H. Saltzmann, *Org. Synth.* 43 (1963) 62–64.
- [41] H.J. Lucas, E.R. Kennedy, M.W. Forno, *Org. Synth.* 43 (1963) 483.
- [42] S. Brunauer, P.H. Emmett, E. Teller, *J. Am. Chem. Soc.* 60 (1938) 309–319.
- [43] J.E.F.C. Gardolinski, G. Lagaly, *Clay Miner.* 40 (2005) 547–556.
- [44] V. Umamaheswari, W. Böhlman, A. Pöpl, A. Vinu, M. Hartmann, *Microporous Mesoporous Mater.* 89 (2006) 47–57.
- [45] A. Jitianu, M. Crisan, A. Meghea, I. Rau, M. Zaharescu, *J. Mater. Chem.* 12 (2002) 1401–1407.
- [46] J.J. Tunney, C. Detellier, *Chem. Mater.* 5 (1993) 747–748.
- [47] K.B. Brandt, T.A. Elbokl, C. Detellier, *J. Mater. Chem.* 13 (2003) 2566–2572.
- [48] J.J. Tunney, C. Detellier, *Can. J. Chem.* 75 (1997) 1766–1772.
- [49] J.E. Gardolinski, P. Peralta-Zamora, F. Wypych, *J. Colloid Interface Sci.* 211 (1999) 137–141.
- [50] K.J. Ciuffi, E.J. Nassar, L.A. Rocha, Z.N. da Rocha, S. Nakagaki, G. Mata, R. Trujillano, M.A. Vicente, S.A. Korili, A. Gil, *Appl. Catal. A* 319 (2007) 153–162.
- [51] J.M. Thomas, R. Raja, G. Sankar, R.G. Bell, *Acc. Chem. Res.* 34 (2001) 191–200.
- [52] R.G. Pearson, *J. Am. Chem. Soc.* 85 (1963) 3533–3543.
- [53] I. Fernandez, J.R. Pedro, A.L. Roselló, R. Ruiz, I. Castro, X. Ottenwaelder, Y. Journaux, *Eur. J. Org. Chem.* 7 (2001) 1235–1247.
- [54] R. Bechara, D. Balloy, J.Y. Dauphin, J. Grimblot, *Chem. Mater.* 11 (1999) 1703–1711.
- [55] U. Schuchardt, W. Carvalho, E.V. Spinacé, *Synlett* 10 (1993) 713–718.
- [56] U. Schuchardt, D. Cardoso, R. Sercheli, R. Pereira, R.S. Da Cruz, M.C. Guerreiro, D. Mandelli, E.V. Spinacé, E.L. Pires, *Appl. Catal. A* 211 (2001) 1–17.
- [57] G.B. Shul'pin, C.C. Golfeto, G. Süß-Fink, L.S. Shul'pina, D. Mandelli, *Tetrahedron Lett.* 46 (2005) 4563–4567.
- [58] G. Dubois, A. Murphy, T.D. Stack, *Org. Lett.* 14 (2003) 2469–2472.
- [59] J.G. Carriazo, M.A. Centeno, J.A. Odriozola, S. Moreno, R. Molina, *Appl. Catal. A: Gen.* 317 (2007) 120–128.
- [60] J.T. Groves, *J. Inorg. Biochem.* 100 (2006) 434–447.
- [61] G. Nizova, B. Krebs, G. Süß-Fink, S. Schindler, L. Westerheide, G.L. Cuervo, B. Shul'pin, *Tetrahedron* 58 (2002) 9231–9237.
- [62] F. Gozzo, *J. Mol. Catal. A: Chem.* 171 (2001) 1–22.
- [63] J.R. Ruiz, C. Jiménez-Sanchidrián, R. Llamas, *Tetrahedron* 63 (2007) 1435–1439.
- [64] A. Steffen, S. Teixeira, J. Sepulveda, R. Rinaldi, U. Schuchardt, *J. Mol. Catal. A: Chem.* 287 (2008) 41–44.